Review Article

Future imaging of atherosclerosis: molecular imaging of coronary atherosclerosis with ^{18}F positron emission tomography

Daniel J. Scherer[1,2,3], Peter J. Psaltis[1,2,3]

[1]Vascular Research Centre, Heart Health Theme, South Australian Health and Medical Research Institute, Adelaide, South Australia 5000, Australia; [2]Royal Adelaide Hospital, South Australia 5000, Australia; [3]School of Medicine, The University of Adelaide, South Australia 5000, Australia

Contributions: (I) Conception and design: All authors; (II) Administrative support: All authors; (III) Provision of study materials or patients: None; (IV) Collection and assembly of data: All authors; (V) Data analysis and interpretation: All authors; (VI) Manuscript writing: All authors; (VII) Final approval of manuscript: All authors.

Correspondence to: Dr. Daniel J. Scherer, MBBS, FRACP. Vascular Research Centre Heart Health Theme, SAHMRI, North Terrace, SA 5000, Australia. Email: Daniel.Scherer@sahmri.com.

Abstract: Atherosclerosis is characterized by the formation of complex atheroma lesions (plaques) in arteries that pose risk by their flow-limiting nature and propensity for rupture and thrombotic occlusion. It develops in the context of disturbances to lipid metabolism and immune response, with inflammation underpinning all stages of plaque formation, progression and rupture. As the primary disease process responsible for myocardial infarction, stroke and peripheral vascular disease, atherosclerosis is a leading cause of morbidity and mortality on a global scale. A precise understanding of its pathogenic mechanisms is therefore critically important. Integral to this is the role of vascular wall imaging. Over recent years, the rapidly evolving field of molecular imaging has begun to revolutionize our ability to image beyond just the anatomical substrate of vascular disease, and more dynamically assess its pathobiology. Nuclear imaging by positron emission tomography (PET) can target specific molecular and biological pathways involved in atherosclerosis, with the application of ^{18}Fluoride PET imaging being widely studied for its potential to identify plaques that are vulnerable or high risk. In this review, we discuss the emergence of ^{18}Fluoride PET as a promising modality for the assessment of coronary atherosclerosis, focusing on the strengths and limitations of the two main radionuclide tracers that have been investigated to date: 2-deoxy-2-(^{18}F)fluoro-D-glucose (^{18}F-FDG) and sodium ^{18}F-fluoride (^{18}F-NaF).

Keywords: Coronary artery disease (CAD); coronary vessels; molecular imaging; positron emission tomography (PET); fluorodeoxyglucose F18; cardiac imaging techniques

Submitted Sep 01, 2015. Accepted for publication Oct 30, 2015.
doi: 10.21037/cdt.2015.12.02
View this article at: http://dx.doi.org/10.21037/cdt.2015.12.02

Introduction

Atherosclerosis is a slowly progressive, chronic disease process characterised by the formation of plaque within arterial walls. It is the underlying pathology of ischaemic heart disease, which is a leading cause of death worldwide accounting for 7.4 million deaths worldwide in 2012 (1). With the increasing rates of obesity and type 2 diabetes, the burden of coronary artery disease (CAD) is expected to continue to rise in future years (2).

Atherosclerosis occurs in the setting of endothelial dysfunction of arteries causing increased endothelial permeability, allowing uptake and retention of apolipoprotein B containing lipids within the subendothelial space. There the lipoproteins can become oxidised and provide an increased stimulation for the overlying endothelium to release chemokines that attract leukocytes. Monocytes transmigrate through the endothelium to enter the subendothelial space where they differentiate into macrophages and take up the retained and modified lipoproteins, eventually becoming lipid laden foam cells. Macrophages can undergo apoptosis

but in the early stages of atherosclerosis these apoptotic cells are cleared by efferocytosis that has an anti-inflammatory and stabilizing effect. Over an extended period of time though the need for recurrent efferocytosis and prolonged exposure of cells within the plaque environment to oxidized low density lipoprotein (LDL) can lead to endoplasmic reticulum stress within macrophages and cause secondary necrosis, releasing their cellular contents and further stimulating the cycle and contributing to the formation of lipid rich plaques within the arterial wall (3-5).

Therefore the underlying pathogenic substrate of atherosclerosis is complex, comprising multiple extracellular, cellular and molecular mediators that participate in a cascade of disordered lipid metabolism, chronic inflammation, cell death, angiogenesis and thrombosis all taking place within the vessel wall.

Despite seminal advances in the field of cardiovascular medicine, the risk of complications from coronary atherosclerosis remains considerable, culminating in the sequelae of myocardial infarction. The ongoing need to optimize risk assessment, prevention and treatment strategies hinges on an improved understanding of the pathogenic basis of CAD. In the clinical setting, there are also the specific needs to be able to identify high risk or "vulnerable" coronary plaques and monitor their responsiveness to therapeutic interventions.

Coronary imaging is central to this. Traditional assessment of coronary atherosclerosis has focused solely on anatomical imaging, evolving over recent decades from conventional coronary angiography to intravascular modalities, such as intravascular ultrasound (IVUS) and optical coherence tomography (OCT) and noninvasive techniques, such as a computed tomography (CT). However, there is now also increasing recognition of the scope for molecular imaging to provide assessment of the biological composition of plaque and characterize the dynamic nature of more vulnerable lesions. In this review, we will direct our focus to the use of positron emission tomography (PET) and the applicability of ^{18}Fluoride-based radionuclide tracers for molecular imaging of coronary atherosclerosis.

"Non-molecular coronary imaging"

Invasive contrast X-ray angiography has been the gold standard for imaging of coronary atherosclerosis over the past 50 years since Dr. F. Mason Sones Jr performed the first selective coronary angiogram by accident in 1958 (6). While remaining the imaging standard and the most studied in regards to patient outcomes, coronary angiography does not provide imaging of atherosclerosis itself, but rather its end result. It has the ability to show the residual coronary lumen and subsequently the degree of stenosis when compared with a reference segment of unaffected vessel, but does not directly visualize plaque or the vessel wall. As a consequence, preservation of the luminal appearance on coronary angiography does not equate to the absence of plaque, and this is particularly true where the vessel wall has undergone positive (or outward) remodeling, as often takes place especially in the early stages of atherogenesis.

The advent of IVUS and subsequent intravascular imaging modalities, such as OCT and near-infrared spectroscopy (NIRS) delivered the ability to directly image the vessel wall and atherosclerotic plaque. These intravascular imaging modalities have progressed our understanding of atherosclerosis significantly and have helped to image plaque at all stages of its development, while also defining its compositional features that are associated with plaque vulnerability. Although invasive, they have also enabled a means by which to serially monitor the natural history of plaque and its modulation with anti-atherosclerotic therapies. While having the ability to identify vulnerable characteristics, such as high plaque volume, thin fibrous cap, lipid-rich core, spotty calcification and intraplaque neovascularization and hemorrhage, they are as yet unable to determine the activity of plaque, in terms of pathogenic molecular pathways. Ideal modalities for imaging of coronary atherosclerosis should combine non-invasiveness so that patients can be assessed at repeat intervals with minimum risk, and the accurate and reproducible ability to identify early signals of plaque vulnerability that predict a high risk of progression and complication.

Molecular imaging

Molecular imaging was christened as a term in the mid to late 1990s to encompass *in vivo* functional imaging modalities, which go beyond anatomical tissue assessment to also visualize and quantify specific biological processes down to a cellular and molecular level. The early progress and focus of development centered on imaging in oncology but has expanded to use throughout medicine (7).

There are a large number of different molecular imaging agents that are able to target a diverse range of biological activity across the spectrum of pathologies in medicine. These typically combine a targeting component, that ideally

interacts specifically with the biochemical process being investigated, and an imaging component that can attach to the targeting component without affecting its interaction with the targeted biochemical process (8). In studies of atherosclerosis unique molecular imaging agents have been created for assessment of a wide variety of processes that contribute to atherogenesis. These have included targeting of vascular cell adhesion molecule-1, monocyte recruitment, macrophage phagocytic activity, apoptosis, oxidative stress, matrix metalloproteinases, intraplaque hemorrhage, and neoangiogenesis (9-11). There are numerous imaging modalities that are used for identification of these imaging agents including PET, single-photon emission CT, magnetic resonance imaging (MRI), and ultrasound, as well as optical imaging modalities including bioluminescence and fluorescence that can be used for *in vivo* animal imaging. Of these the most promising at a clinical level are MRI and PET.

Positron emission tomography (PET)

PET scanning was first described clinically in the 1950s. Positron emission decay occurs when a proton is turned into a neutron with the release of a positron and a neutrino. The combination of a positron and an electron results in an annihilation reaction which produces two 511 keV photons that are emitted in approximate opposite direction to each other. This release allows identification of positron emission when detectors on opposite sides of the body record simultaneous detection, only registering those that co-detect within a few nanoseconds (12). PET and CT scans have been combined since the 1990s allowing the functional information obtained by PET to be more precisely located anatomically and three dimensionally reconstructed when co-localized with CT images (13).

There are a number of positron emitting isotopes including Carbon 11, Nitrogen 13, Oxygen 15, Gallium 68, Rubidium 82 and Fluorine 18 (^{18}F). The most common in use in medical imaging is ^{18}F, which is produced in a cyclotron by bombarding Oxygen 18 enriched water with high energy protons and has a half-life of 109.77 minutes (12). ^{18}F labeling is used as the imaging component in a number of investigational molecular imaging agents, including [^{18}F]Galacto-RGD in angiogenesis, [^{18}F]P2,P3-monochloromethylene diadenosine-5',5"'-P1,P4-tetraphosphate in plaque inflammation, and ^{18}F-Fluoromisonadazole in hypoxia (11). This review will focus however on the two most commonly used ^{18}F labelled isotopes, ^{18}F-FDG and sodium ^{18}F-fluoride (^{18}F-NaF).

2-deoxy-2- (^{18}F) fluoro-D-glucose (^{18}F-FDG)

2-deoxy-2- (^{18}F)fluoro-D-glucose or ^{18}F-FDG has become the most commonly used radiotracer in the world and a mainstay of imaging in oncology. ^{18}F-FDG is a radiolabelled analogue of glucose that enters cells via the same receptors, the GLUT family of transporters. Once ^{18}F-FDG has entered cells it is phosphorylated by hexokinase, metabolically trapping it within the cell. Accumulation of intracellular ^{18}F-FDG is also contributed to by the absence of the hydroxyl group at the 2' position affecting its ability to undergo further metabolism along the glycolytic pathway (14).

The use of ^{18}F-FDG in oncology is based on the increased metabolic demand and subsequent glycolysis of tumor cells that use glucose as their source of energy. ^{18}F-FDG PET was adopted rapidly for cancer imaging and was initially thought to potentially be a specific imaging modality that would allow not only monitoring of malignancy but also a tool to help differentiate it from other pathologies. However, this proved not to be the case, with ^{18}F-FDG uptake also seen in both benign conditions and in the setting of inflammation (15-18).

Inflammatory basis of atherosclerosis

Inflammation plays a central role in atherosclerosis. Activated intimal endothelial cells express P-selectin and cell adhesion molecules, which in turn recruit circulating leukocytes, such as monocytes that express P-selectin glycoprotein ligand-1 (PSGL-1). These cells adhere to and roll on the endothelium (19). PSGL-1 expressing leukocytes are thought to be a pro-inflammatory subset containing large amounts of pro-inflammatory cytokines. Macrophages differentiate from monocytes at the sites of plaque, and are capable of releasing a large array of cytokines including IL-1, IL-6, IL-12, IL-15, IL-18, and TNF alpha (20), propagating further inflammation at these sites of early atherogenesis. This continues throughout the natural history of the plaque with attraction and accumulation of monocytes at the site of plaques continuing throughout and in a manner proportional to plaque size (21). Monocytes and macrophages are the most abundant leukocyte involved in atherogenesis but others, including neutrophils, T and B cells, also contribute to promoting inflammation both directly and by co-stimulatory interaction between themselves (20,22). Oxidized subendocardial LDL contributes to the formation of foam cells from macrophages, and to the inflammatory milieu

of atherosclerosis. Its presence also induces the secretion of potent chemokines, such as CCL2, in endothelial and smooth muscle cells (23,24) and stimulates the production of reactive oxygen species and prostaglandins by macrophages, and other inflammatory cells (25,26).

Acute rupture of atherosclerotic plaque is a common cause of acute myocardial infarction, occurring in 60-80% of acute coronary syndrome (ACS) cases, and is found in the majority of cases of sudden cardiac death with intraluminal thrombi (27,28). Plaque vulnerability and rupture has a strong association with inflammation (29). Macrophages are found in highest concentration in vulnerable atherosclerotic plaques and contribute to the thinning of the fibrous plaque cap by release of matrix metalloproteinases, making them more likely to rupture (30-35). The critical involvement of macrophages in plaque development and disruption makes them an obvious imaging target for the early identification of vulnerable plaques before complications arise.

^{18}F-FDG detection of vascular inflammation

Both macrophages and foam cells have been shown *in vitro* to take up ^{18}F-FDG and at a comparable level to some cancer cell lines (34,36,37). Initially the uptake of ^{18}F-FDG in atherosclerotic plaque was thought to be due to the respiratory burst of macrophages when phagocytizing the subendothelial oxidized LDL particles (38,39). However, Folco *et al*. showed that hypoxia is the main driver that modulates glucose uptake in macrophages, mediated by increased expression of hexokinase-2 rather than upregulation of the GLUT1 transporter (40). Hypoxia is a prominent feature of the atherosclerotic milieu and associates strongly with the burden of macrophage infiltration and inflammation (41). Animal (42-48) and human (33,49-51) studies have consistently demonstrated a correlation between ^{18}F-FDG uptake and the presence and density of macrophages in atherosclerosis.

^{18}F-FDG PET vascular imaging in humans was first described in 1999 in Takayasu's arteritis, before being investigated in other vasculitides (52-54). However, case studies subsequently noted vascular uptake even in the absence of vasculitis (55). Retrospective analysis of ^{18}F-FDG PET scans in patients undergoing oncological workup identified vessel wall uptake in as many as 50% (56). In a number of cases this uptake was nonuniform along the length of the vessel and in one case where uptake extended from the abdominal aorta to the femoral arteries, it was recognized that this corresponded to extensive atherosclerotic disease seen also on CT imaging. A study by Yun *et al*. then drew associations between ^{18}F-FDG uptake in large arteries and the presence of cardiovascular risk factors and documented CAD (57).

These observational results paved the way for more dedicated assessment of ^{18}F-FDG imaging for atherosclerosis. The potential of ^{18}F-FDG PET was demonstrated early on in a rabbit model of atherosclerosis in which an intravascular positron sensitive probe was used (43). In 2002 Rudd and colleagues then reported a ^{18}F-FDG PET study performed in eight patients with symptomatic carotid artery disease (49). All patients displayed ^{18}F-FDG uptake in the symptomatic carotid stenosis, and the mean signal was 27% higher than that observed in the asymptomatic contralateral stenosis present in six of them. Histological assessment of the endarterectomized arteries also confirmed heavy macrophage infiltration at the ^{18}F-FDG positive sites.

Patients with known CAD have a high prevalence of carotid artery uptake of ^{18}F-FDG and known cardiovascular risk factors including elevated body mass index, age >65 years, hypertension, and smoking, have been shown to be both strong determinants and independent predictors of vascular ^{18}F-FDG uptake (58). Retrospective analyses have suggested correlation of ^{18}F-FDG vascular uptake with increased risk for cardiovascular events (59). Meanwhile prospective studies in patients with symptomatic carotid artery disease have shown that high levels of ^{18}F-FDG uptake predict early stroke recurrence for both symptomatic and asymptomatic carotid lesions (60-63).

^{18}F-FDG imaging of coronary atherosclerosis

Coronary artery uptake had been noted in studies looking retrospectively at ^{18}F-FDG PET scans. In 2009 the first prospective study of coronary uptake was performed, comparing culprit lesion stent sites in 10 ACS and 15 stable CAD patients, as well as in recent to remote stent sites in the stable CAD group (64). Uptake in ACS plaques quantified by the target-to-background ratio (TBR) was higher than in stable CAD plaques (2.61 *vs*. 1.74, P=0.02), while no significant difference was found between recent and remote stent sites (1.74 *vs*. 1.43, P=0.49), suggesting that ^{18}F-FDG signal correlated with acute plaque features, and not simply to post-angioplasty changes (64).

^{18}F-FDG imaging has been shown to be highly reproducible over short interscan time periods (65) and also to be able to identify plaque changes in plaque regression studies with serial imaging in rabbits (66). It has been used

as a serial imaging tool in multiple small intervention trials in humans using statins, and pioglitazone (67,68) Another of its applications has been to confirm that new pharmaceutical agents undergoing clinical evaluation do not cause adverse inflammatory effect on blood vessels, as implemented in the dal-PLAQUE study where dalcetrapib was shown not to be proinflammatory or proatherogenic after concerns had been raised about cholesteryl ester transfer protein inhibitors as a group after the failure of torcetrapib due to off target effects (69,70).

Together these longitudinal studies that have been conducted over relatively short intervals, 3 months, have shown the potential for ^{18}F-FDG PET coronary imaging to provide surrogate assessment of the effectiveness of anti-atherogenic interventions. This in turn can help guide decision making for clinical research programs to determine which therapies are worth investigating in larger and longer phase III trials which measure hard clinical outcomes. Some retrospective analyses of oncological patients undergoing multiple ^{18}F-FDG PET scans over longer interscan periods with no specific plaque stabilising intervention however have shown zero correlation between plaque uptake between scans, potentially questioning its ability to serially monitor atherosclerotic plaque in longer duration studies (71).

A major limitation of ^{18}F-FDG based imaging of coronary atherosclerosis relates to the background noise created by ^{18}F-FDG uptake in the adjacent myocardium. When combined with PET's fundamental limitation of spatial resolution (4.2–6.3 millimeters) contributed to by detector size, positron emission range, and non-collinearity, the ability for PET to be able to differentiate between coronary artery and myocardium significantly effects its ability to identify true coronary signal (72,73). While efforts have been made to reduce background myocardial uptake, for example by providing a low carbohydrate-high fat diet prior to scan acquisition (74), the rate of uninterpretable scans in human patients remains prohibitively high. Thus far this has significantly limited the accuracy and reproducibility of coronary ^{18}F-FDG PET in the rigorous setting of clinical trials, while also precluding its wider application in routine clinical practice.

Another issue that needs to be considered in assessing the PET/CT assessment of coronary atherosclerosis is the radiation exposure to the patient with this imaging modality. With modern day combination scanners a PET/CT cardiac scan exposes patients to a radiation dose in the order of 8-11mSv, with the majority of this accounted for by the internal exposure from the ^{18}F (75).

Sodium ^{18}F-fluoride (^{18}F-NaF)

^{18}F-Fluoride has been used as a radionuclide for bone scanning since the 1960's (76). Fluoride is well known to be taken up by bone mineral with the main body store of fluoride thought to be the skeleton (77), with exchange of fluoride for one of the hydroxyl ions of hydroxyapatite forming fluorapatite the purported mechanism of skeletal ^{18}F-NaF uptake (78). For a period of time ^{18}F-NaF was superseded by technetium-based radiotracer compounds that had superior characteristics for imaging with gamma cameras. However, the advent of PET scanner technology and its well-established place in oncological practice has seen the re-emergence of ^{18}F-NaF. In particular, it has been widely used for the assessment of multiple types of bone pathology and increasingly for bone metastases (79). Notably, its uptake on PET scanning has been shown to correlate with dynamic indexes of bone formation (80).

^{18}F-NaF, vascular calcification and cardiovascular risk

Vascular calcification occurs as an active process in atherosclerosis and is seen with increasing frequency with advancing age and also with increasing atherosclerotic burden (81). Osteogenic differentiation of different cell populations present in the vessel wall, including medial smooth muscle cells and adventitial fibroblasts, pericytes, and mesenchymal stem cells, is stimulated in the inflammatory milieu of atherosclerosis. Macrophages within atherosclerotic plaque promote osteogenesis by the release of cytokines (e.g., IL-1, IL-6, IL-8, tumor necrosis factor alpha, insulin-like growth factor-1, and transforming growth factor-beta) (82-85). Once established the presence of microcalcification crystals contributes to a positive feedback loop by inducing a pro-inflammatory response in macrophages that further propagates the pro-calcific stimulus in the vessel wall (86). Formation and progression of vascular calcification is very similar to bone formation, with the generation of hydroxyapatite crystals in the vessel wall. Given the similarities to bone formation, it is intuitive that vascular calcification may be an amenable target for molecular imaging with ^{18}F-NaF.

Several retrospective studies have observed ^{18}F-NaF uptake within the vasculature of patients who have undergone full body ^{18}F-NaF PET imaging to detect bony metastases in the setting of malignancy (*Table 1*). Derlin *et al.* first reported this phenomenon in 76% of 75 patients undergoing radionuclide imaging for bone metastases, with

Table 1 Clinical studies of atherosclerosis with ^{18}F-NaF PET

Study	Site	Design	Patient number	Dose	Uptake period	Prevalence	Comments	Results
Derlin *et al*. (87)	Major arteries	Retrospective	75	350±50 MBq	60 min	57/75 (76%)	First feasibility study	Correlation between ^{18}F-NaF uptake and AC
Derlin *et al*. (88)	Carotid artery	Retrospective	269	350±50 MBq	60 min	94/269 (35%)	Comparison of ^{18}F-NaF uptake to CV RFs	Male, age, HT, ↑ chol correlated with ^{18}F-NaF uptake; ↑ prevalence of ^{18}F-NaF uptake with ↑ RFs
Derlin *et al*. (89)	Major arteries	Retrospective	45	350±50 MBq	60 min	27/45 (60%)	Comparison of ^{18}F-NaF and ^{18}F-FDG	^{18}F-NaF more likely to co-localize with AC; co-uptake only seen in 6.5% of lesions
Li *et al*. (90)	Major arteries + coronary arteries	Retrospective	61	370±74 MBq	40 min	59/61 (97%)	First study to assess coronary arteries	↑ Coronary ^{18}F-NaF uptake with Hx of CV event (SUV 1.70 *vs*. 1.39, P=0.029)
Beheshti *et al*. (91)	Combined myocardium/ coronary arteries + aorta	Retrospective	59	370-550 MBq	60 min	Not described	Trialled new technique assessing ROI including both myocardium & coronary arteries (GMCS)	↑ ^{18}F-NaF uptake with age
Dweck *et al*. (92)	Coronary arteries	Prospective	119	125 MBq	60 min	34%	Comparison of ^{18}F-NaF and ^{18}F-FDG	^{18}F-NaF but not ^{18}F-FDG correlated with ↑ Framingham risk scores; no ^{18}F-NaF uptake in 41% with CAC >1,000
Kurata *et al*. (93)	Major arteries	Retrospective	29	~185 MBq	60 min	8/29 (28%)	Uptake was not corrected for blood pooling	91% of ^{18}F-NaF co-localized to AC but only 10% of all AC had ^{18}F-NaF uptake
Janssen *et al*. (94)	Femoral arteries	Retrospective	409	350±50 MBq	60 mins	159/409 (39%)		^{18}F-NaF correlated with Age, HT, ↑ Chol, DM, Hx of smoking, Hx of CV events; ↑ prevalence of ^{18}F-NaF uptake with ↑ RFs
Blomberg *et al*. (95)	Coronary arteries + thoracic aorta	Prospective	38	2.2 MBq/kg	45, 90 & 180 mins	Not described	Assessment of delayed image acquisition points	Blood pool corrected uptake not affected over time
Joshi *et al*. (96)	Coronary arteries (carotid arteries)	Prospective	80 (+9 carotid patients)	125 MBq	60 mins	37/40 (93%) in ACS group; 32/40 (80%) in stable CAD group	Comparison between ^{18}F-NaF *vs*. ^{18}F-FDG and ACS *vs*. stable CAD	34% higher TBR in ACS plaques; 93% (NaF) *vs*. 33% (FDG) uptake in culprit vessels
Morbelli *et al*. (97)	Major arteries	Retrospective	80	370 MBq	60 mins	Not described	Comparison between ^{18}F-NaF uptake and CT calcification as assessed by Framingham risk factors	^{18}F-NaF uptake dependent on age, HT; smoking & DM; calcification dependent only on age
Fiz *et al*. (98)	Infra-renal abdominal aorta	Prospective	64	4.8–5.2 MBq/kg	60–75 mins	Not described	Comparison between ^{18}F-NaF uptake to density of calcification	Inverse correlation between ^{18}F-NaF uptake and density of calcification

AC, arterial calcification; ACS, acute coronary syndrome; CAC, coronary artery calcification score; CAD, coronary artery disease; CT, computed tomography; CV, cardiovascular; DM, diabetes mellitus; GMCS, global molecular calcification score; HT, hypertension; RFs, risk factors; ROI, region of interest.

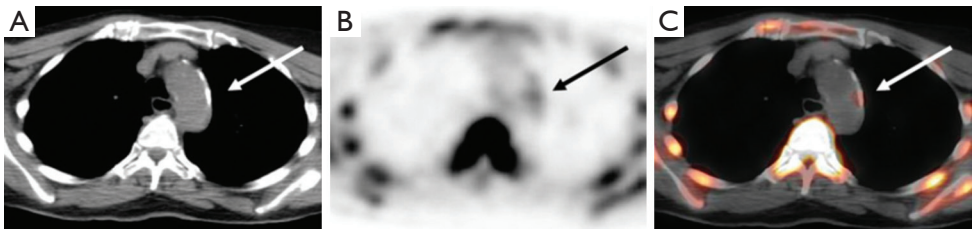

Figure 1 ^{18}F-sodium fluoride PET/CT images of the aortic arch. (A) CT image; (B) PET image; (C) fused PET/CT image. ^{18}F-sodium fluoride uptake in this atherosclerotic lesion coincided with calcification on CT imaging (arrows). Reproduced from "Feasibility of ^{18}F-sodium fluoride PET/CT for imaging of atherosclerotic plaque." Derlin T, Richter U, Bannas P, *et al.* J Nucl Med 2010;51:862-5. © by the Society of Nuclear Medicine and Molecular Imaging, Inc. PET, positron emission tomography; CT, computed tomography.

the most common arterial sites of ^{18}F-NaF uptake being the femoral arteries and aorta (87). In 95% of these cases, arterial wall calcification was confirmed by CT assessment also (*Figure 1*).

Other retrospective studies of similar patient populations have described association between the incidence of ^{18}F-NaF uptake in the peripheral vasculature and the number of cardiovascular disease risk factors and variations of Framingham cardiovascular risk scores (88,94,97). In one particular study ^{18}F-FDG and ^{18}F-NaF PET were compared retrospectively in a group of 45 patients who had undergone both types of assessment for oncological work up (89). ^{18}F-NaF showed a markedly increased propensity for co-localization with vascular calcification than did ^{18}F-FDG (77.1% *vs.* 14.5%), with co-localization of both radiotracers at the same site present in only 6.5% of cases.

^{18}F-NaF and coronary atherosclerosis

Dweck *et al.* performed the first prospective trial focused specifically on assessment of ^{18}F-NaF uptake in coronary arteries as a substudy of a trial that investigated PET imaging of aortic stenosis (99). 119 patients were studied, including a control group of 13 who had no history of CAD or CT evidence of coronary artery calcification. Each patient underwent PET imaging with both ^{18}F-FDG and ^{18}F-NaF as a radiotracer in separate scans. Uptake of ^{18}F-NaF but not ^{18}F-FDG was found to be higher in patients with CAD compared to the control group (1.64±0.49 *vs.* 1.23±0.24, P=0.003 for ^{18}F-NaF; 1.18±0.31 *vs.* 1.23±0.20, P=0.498 for ^{18}F-FDG). Although significant correlations were found between ^{18}F-NaF uptake and both Framingham risk score and coronary artery calcification, 41% of patients with coronary artery calcium scores >1,000 had no significant radiotracer uptake. Of particular interest were the findings in one patient who had suffered a recent myocardial infarction. Despite the presence of coronary artery calcification of all three coronary arteries, ^{18}F-NaF was seen only at the site of the culprit lesion (92).

This finding prompted the same investigators to perform a comparison of ^{18}F-NaF and ^{18}F-FDG PET imaging of coronary arteries in patients presenting with ACS and those undergoing elective percutaneous coronary intervention for stable angina (96). Measuring TBR for ^{18}F-NaF, they showed a 34% higher activity in culprit versus non-culprit plaques (maximum TBR 1.66 *vs.* 1.24, P<0.0001), with 93% of the culprit plaques showing ^{18}F-NaF uptake. By comparison assessment of ^{18}F-FDG signal in the coronary arteries was affected by background myocardial noise in half the patients, despite preparation with a low carbohydrate-high fat diet, such that the two could not be distinguished. In those patients in whom this was not the case (n=18), ^{18}F-FDG uptake could only be detected in a third of culprit vessels, and there was no difference in TBR compared to non-culprit lesion sites (1.71 *vs.* 1.58, P=0.34). Although the cohort of patients with stable angina had more extensive CAD than the ACS group, with more arterial calcification, ^{18}F-NaF uptake was seen in less than half of this group and did not correlate with the sites of stent deployment but rather more often coincided with non-obstructive lesions of <70% stenotic severity. Further analysis with VH-IVUS in the patients revealed that coronary plaques with ^{18}F-NaF uptake were more likely to contain vulnerable plaque characteristics, such as positive remodeling, microcalcification, and necrotic core (100,101).

Taken together, these results indicate that the expectation that ^{18}F-NaF uptake correlates with gross arterial calcification does not hold true. Another recent study that set out to specifically address this hypothesis in fact showed that ^{18}F-NaF coronary signal correlated inversely with coronary calcium density, as classified in tertiles of light (130 to 210 HU), medium (211 to 510 HU), or heavy (>510 HU)

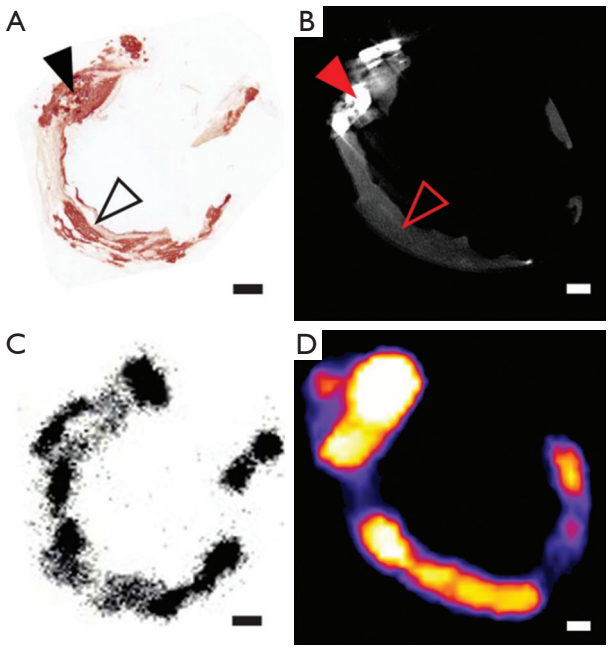

Figure 2 Sections showing macrocalcification (solid arrow) and microcalcification (hollow arrow) in: (A) histology section with Alizarin Red staining; (B) micro CT; (C) autoradiography; (D) ^{18}F-NaF microPET. Adapted from original publication in *Nature Communications* "Identifying active vascular microcalcification by 18F-sodium fluoride positron emission tomography." Irkle A, Vesey AT, Lewis DY, *et al.* Nat Commun 2015;6:7495. Licensed under CC BY 4.0. PET, positron emission tomography; CT, computed tomography.

calcification on CT imaging (98). Rather, the above data start to build a compelling case that ^{18}F-NaF signal in the coronary vasculature more frequently associates with plaques that are actively inflamed and responsible for ACS events. Importantly, it does so to a far greater extent than ^{18}F-FDG, without its detection being compromised by the same limitations caused by background myocardial noise.

Basis for ^{18}F-NaF uptake in unstable plaque: microcalcification

Given what is known about uptake of ^{18}F-NaF in bone, active microcalcification in atherosclerotic plaque appears to be the most likely substrate for ^{18}F-NaF uptake in the vasculature. However, owing to a paucity of cellular and animal model studies, the exact molecular mechanisms for this remain unclear.

The most insightful information regarding the mechanism of ^{18}F-NaF vascular uptake comes from an elegant study, recently published by Irkle *et al.* who performed comprehensive examinations of human carotid artery lesions *in vivo* and *ex vivo* (102). Pharmacokinetic and pharmacodynamic analysis confirmed favourable properties of ^{18}F-NaF for arterial plaque assessment, including its high affinity for calcification, no significant dissociation from its target within standard time to scans, and low plasma activity at the time of scanning meaning minimal background noise. With the use of a microprobe and scanning electron microscope, fluoride and calcification were identified in carotid tissue. The presence of fluoride was found to be highly specific to calcification and more commonly co-localized with microcalcifications than macrocalcifications.

CT scanning (both micro and clinical) was able to reliably identify macrocalcification but not areas of microcalcification. In contrast, ^{18}F-NaF PET showed uptake in areas that were not identified on CT and these corresponded to sites of microcalcification detected by Alizarin Red staining of contiguous histological sections (*Figure 2*). The same study also assessed the possibility that ^{18}F-NaF uptake could be due to other inflammatory processes at the site of atherosclerosis that precede and contribute to active calcification. However, unlike the strong correlation seen with Alizarin Red staining for mineralisation, ^{18}F-NaF signal correlated poorly with immunohistochemical detection of macrophage infiltration, or the presence of endothelial or smooth muscle cells (*Figure 3*).

Vascular macrocalcification on CT scanning is well established as a predictor of cardiovascular events but does not specifically identify vulnerable plaques (103). However, recent data from CT and IVUS-based studies have indicated that macrocalcification may in fact be protective against acute coronary events (104,105). Conversely, microcalcification is increasingly well understood to be a specific feature of vulnerable plaque, making its detection highly desirable in atherosclerosis imaging (106). As evident from the aforementioned studies, ^{18}F-NaF PET is more sensitive and accurate than either ^{18}F-FDG scanning or CTCA in the identification of microcalcification. Therefore it may have utility for the early detection of vulnerable plaque in high risk patients.

Future directions

Further studies are needed to more comprehensively delineate the biological and clinical significance of ^{18}F-NaF uptake in coronary atheroma and confirm its accuracy and

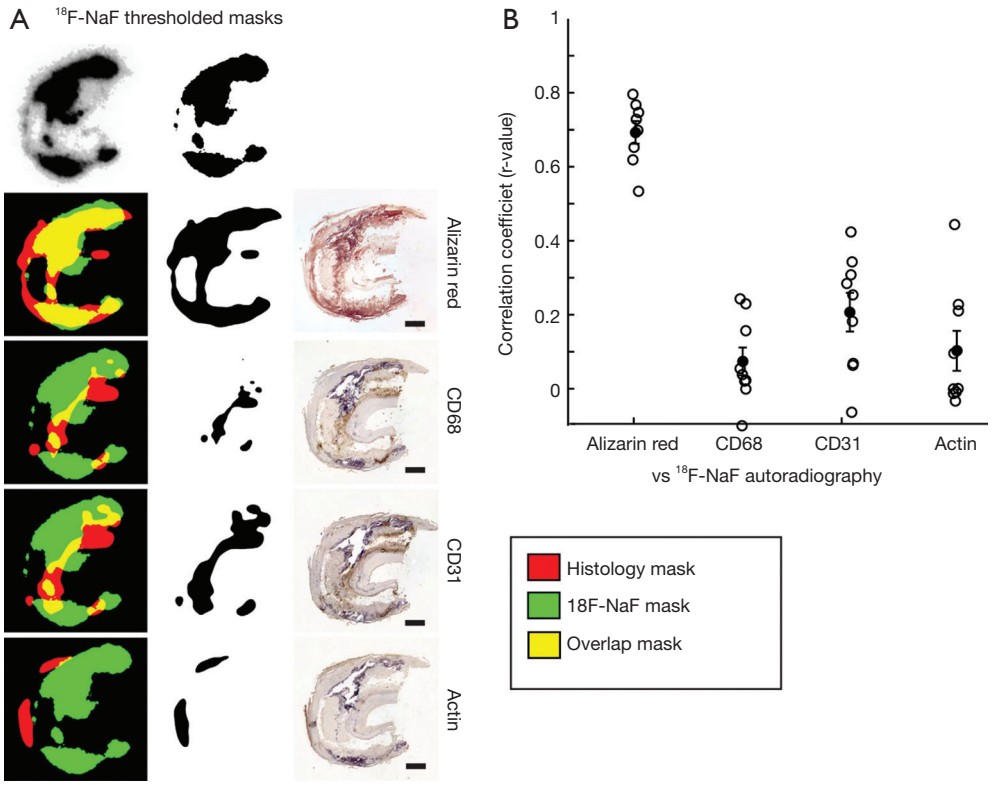

Figure 3 ^{18}F-NaF uptake correlates with calcification but none of the histological inflammatory markers. (A) Representative images of ^{18}F-NaF autoradiography signal overlap with IHC-stained sequential sections. Green: ^{18}F-NaF signal; red: histology signal; yellow: overlap. Scale bar, 1 mm; (B) high correlation is observed between ^{18}F-NaF and alizarin red calcification staining, while low correlation is seen between ^{18}F-NaF autoradiography and inflammatory marker IHC signals. Reproduced from "Identifying active vascular microcalcification by ^{18}F-sodium fluoride positron emission tomography." Irkle A, Vesey AT, Lewis DY, *et al*. Nat Commun 2015;6:7495. Licensed under CC BY 4.0.

reproducibility for identifying vulnerable lesions at high risk of rupture and thrombotic complication. To this regard Newby and collaborators are due to commence recruitment in the Prediction of Recurrent Events With ^{18}F-Fluoride (PREFFIR) study in August 2015 (www.ClinicalTrials.gov NCT02278211). This will aim to recruit 700 ACS patients and undertake both ^{18}F-NaF PET and CTCA for an observational study with cardiac death or recurrent MI as the primary outcome measure assessed for 4 years from study commencement.

There also remains the prospect with ^{18}F-NaF PET imaging for serial, noninvasive monitoring of atherosclerotic lesions over time to delineate the natural history of plaques and assess their responsiveness to different anti-atherosclerotic treatments.

Conclusions

The use of molecular imaging for assessment of coronary atherosclerosis with ^{18}F PET appears a promising tool for the non-invasive identification of vulnerable plaque. This, coupled with ^{18}F-NaF PET's newly described ability to identify microcalcification in plaque, indicates its potential to provide biological characterization of coronary atherosclerosis that is complementary to other non-invasive imaging modalities, such as CTCA. The findings of recent ^{18}F-NaF studies suggest its superiority over ^{18}F-FDG and indicate that it is the more likely radioisotope to be incorporated into future trials. While further investigations are required to more clearly define the utility of ^{18}F PET in routine clinical practice, it potentially will play a major role in future imaging of coronary atherosclerosis.

Acknowledgements

Funding: Dr. Scherer is supported by the Royal Adelaide Hospital A.R. Clarkson scholarship. Dr. Psaltis receives

funding from the National Health and Medical Research Council (PG1086796) and Heart Foundation (FLF100412) of Australia.

Footnote

Conflicts of Interest: The authors have no conflicts of interest to declare.

References

1. World Health Organisation. The top 10 causes of death. Available online: http://www.who.int/mediacentre/factsheets/fs310/en/
2. Laslett LJ, Alagona P Jr, Clark BA 3rd, et al. The worldwide environment of cardiovascular disease: prevalence, diagnosis, therapy, and policy issues: a report from the American College of Cardiology. J Am Coll Cardiol 2012;60:S1-49.
3. Ley K, Miller YI, Hedrick CC. Monocyte and macrophage dynamics during atherogenesis. Arterioscler Thromb Vasc Biol 2011;31:1506-16.
4. Tabas I. Macrophage death and defective inflammation resolution in atherosclerosis. Nat Rev Immunol 2010;10:36-46.
5. Fuster V. Lewis A. Conner Memorial Lecture. Mechanisms leading to myocardial infarction: insights from studies of vascular biology. Circulation 1994;90:2126-46.
6. Ryan TJ. The coronary angiogram and its seminal contributions to cardiovascular medicine over five decades. Circulation 2002;106:752-6.
7. Hoffman JM, Gambhir SS. Molecular imaging: the vision and opportunity for radiology in the future. Radiology 2007;244:39-47.
8. James ML, Gambhir SS. A molecular imaging primer: modalities, imaging agents, and applications. Physiol Rev 2012;92:897-965.
9. Libby P, Nahrendorf M, Weissleder R. Molecular imaging of atherosclerosis: a progress report. Tex Heart Inst J 2010;37:324-7.
10. Quillard T, Libby P. Molecular imaging of atherosclerosis for improving diagnostic and therapeutic development. Circ Res 2012;111:231-44.
11. Temma T, Saji H. Radiolabelled probes for imaging of atherosclerotic plaques. Am J Nucl Med Mol Imaging 2012;2:432-47.
12. Basu S, Hess S, Nielsen Braad P-E, et al. The Basic Principles of FDG-PET/CT Imaging. PET Clin 2014;9:355-70.
13. Townsend DW. Combined PET/CT: the historical perspective. Semin Ultrasound CT MR 2008;29:232-5.
14. Gallagher BM, Fowler JS, Gutterson NI, et al. Metabolic trapping as a principle of oradiopharmaceutical design: some factors resposible for the biodistribution of [18F] 2-deoxy-2-fluoro-D-glucose. J Nucl Med 1978;19:1154-61.
15. Strauss LG. Fluorine-18 deoxyglucose and false-positive results: a major problem in the diagnostics of oncological patients. Eur J Nucl Med 1996;23:1409-15.
16. Shreve PD, Anzai Y, Wahl RL. Pitfalls in oncologic diagnosis with FDG PET imaging: physiologic and benign variants. Radiographics 1999;19:61-77; quiz 150-1.
17. Yamada S, Kubota K, Kubota R, et al. High accumulation of fluorine-18-fluorodeoxyglucose in turpentine-induced inflammatory tissue. J Nucl Med 1995;36:1301-6.
18. Sugawara Y, Gutowski TD, Fisher SJ, et al. Uptake of positron emission tomography tracers in experimental bacterial infections: a comparative biodistribution study of radiolabeled FDG, thymidine, L-methionine, 67Ga-citrate, and 125I-HSA. Eur J Nucl Med 1999;26:333-41.
19. An G, Wang H, Tang R, et al. P-selectin glycoprotein ligand-1 is highly expressed on Ly-6Chi monocytes and a major determinant for Ly-6Chi monocyte recruitment to sites of atherosclerosis in mice. Circulation 2008;117:3227-37.
20. Legein B, Temmerman L, Biessen EA, et al. Inflammation and immune system interactions in atherosclerosis. Cell Mol Life Sci 2013;70:3847-69.
21. Swirski FK, Pittet MJ, Kircher MF, et al. Monocyte accumulation in mouse atherogenesis is progressive and proportional to extent of disease. Proc Natl Acad Sci U S A 2006;103:10340-5.
22. Bäck M, Weber C, Lutgens E. Regulation of atherosclerotic plaque inflammation. J Intern Med 2015;278:462-82.
23. Charo IF, Ransohoff RM. The many roles of chemokines and chemokine receptors in inflammation. N Engl J Med 2006;354:610-21.
24. Daly C, Rollins BJ. Monocyte chemoattractant protein-1 (CCL2) in inflammatory disease and adaptive immunity: therapeutic opportunities and controversies. Microcirculation 2003;10:247-57.
25. Maiolino G, Rossitto G, Caielli P, et al. The role of oxidized low-density lipoproteins in atherosclerosis: the myths and the facts. Mediators Inflamm 2013;2013:714653.
26. Bae YS, Lee JH, Choi SH, et al. Macrophages generate

reactive oxygen species in response to minimally oxidized low-density lipoprotein: toll-like receptor 4- and spleen tyrosine kinase-dependent activation of NADPH oxidase 2. Circ Res 2009;104:210-8, 21p following 218.
27. Virmani R, Kolodgie FD, Burke AP, et al. Lessons from sudden coronary death: a comprehensive morphological classification scheme for atherosclerotic lesions. rterioscler Thromb Vasc Biol 2000;20:1262-75.
28. Hansson GK, Libby P, Tabas I. Inflammation and plaque vulnerability. J Intern Med 2015;278:483-93.
29. Muller JE, Abela GS, Nesto RW, et al. Triggers, acute risk factors and vulnerable plaques: the lexicon of a new frontier. J Am Coll Cardiol 1994;23:809-13.
30. Davies MJ, Richardson PD, Woolf N, et al. Risk of thrombosis in human atherosclerotic plaques: role of extracellular lipid, macrophage, and smooth muscle cell content. Br Heart J 1993;69:377-81.
31. Galis ZS, Sukhova GK, Kranzhöfer R, et al. Macrophage foam cells from experimental atheroma constitutively produce matrix-degrading proteinases. Proc Natl Acad Sci U S A 1995;92:402-6.
32. Libby P. The molecular mechanisms of the thrombotic complications of atherosclerosis. J Intern Med 2008;263:517-27.
33. Tawakol A, Migrino RQ, Bashian GG, et al. In vivo 18F-fluorodeoxyglucose positron emission tomography imaging provides a noninvasive measure of carotid plaque inflammation in patients. J Am Coll Cardiol 2006;48:1818-24.
34. Ogawa M, Nakamura S, Saito Y, et al. What can be seen by 18F-FDG PET in atherosclerosis imaging? The effect of foam cell formation on 18F-FDG uptake to macrophages in vitro. J Nucl Med 2012;53:55-8.
35. Raffel OC, Tearney GJ, Gauthier DD, et al. Relationship between a systemic inflammatory marker, plaque inflammation, and plaque characteristics determined by intravascular optical coherence tomography. Arterioscler Thromb Vasc Biol 2007;27:1820-7.
36. Kubota R, Yamada S, Kubota K, et al. Intratumoral distribution of fluorine-18-fluorodeoxyglucose in vivo: high accumulation in macrophages and granulation tissues studied by microautoradiography. J Nucl Med 1992;33:1972-80.
37. Deichen JT, Prante O, Gack M, et al. Uptake of [18F] fluorodeoxyglucose in human monocyte-macrophages in vitro. Eur J Nucl Med Mol Imaging 2003;30:267-73.
38. Paik JY, Lee KH, Choe YS, et al. Augmented 18F-FDG uptake in activated monocytes occurs during the priming process and involves tyrosine kinases and protein kinase C. J Nucl Med 2004;45:124-8.
39. Nguyen-Khoa T, Massy ZA, Witko-Sarsat V, et al. Oxidized low-density lipoprotein induces macrophage respiratory burst via its protein moiety: A novel pathway in atherogenesis? Biochem Biophys Res Commun 1999;263:804-9.
40. Folco EJ, Sheikine Y, Rocha VZ, et al. Hypoxia but not inflammation augments glucose uptake in human macrophages: Implications for imaging atherosclerosis with 18fluorine-labeled 2-deoxy-D-glucose positron emission tomography. J Am Coll Cardiol 2011;58:603-14.
41. Sluimer JC, Gasc JM, van Wanroij JL, et al. Hypoxia, hypoxia-inducible transcription factor, and macrophages in human atherosclerotic plaques are correlated with intraplaque angiogenesis. J Am Coll Cardiol 2008;51:1258-65.
42. Silvola JM, Saraste A, Laitinen I, et al. Effects of age, diet, and type 2 diabetes on the development and FDG uptake of atherosclerotic plaques. JACC Cardiovasc Imaging 2011;4:1294-301.
43. Lederman RJ, Raylman RR, Fisher SJ, et al. Detection of atherosclerosis using a novel positron-sensitive probe and 18-fluorodeoxyglucose (FDG). Nucl Med Commun 2001;22:747-53.
44. Ogawa M, Ishino S, Mukai T, et al. (18)F-FDG accumulation in atherosclerotic plaques: immunohistochemical and PET imaging study. J Nucl Med 2004;45:1245-50.
45. Zhang Z, Machac J, Helft G, et al. Non-invasive imaging of atherosclerotic plaque macrophage in a rabbit model with F-18 FDG PET: a histopathological correlation. BMC Nucl Med 2006;6:3.
46. Hyafil F, Cornily JC, Rudd JH, et al. Quantification of inflammation within rabbit atherosclerotic plaques using the macrophage-specific CT contrast agent N1177: a comparison with 18F-FDG PET/CT and histology. J Nucl Med 2009;50:959-65.
47. Toczek J, Broisat A, Perret P, et al. Periaortic brown adipose tissue as a major determinant of [18F]-fluorodeoxyglucose vascular uptake in atherosclerosis-prone, apoE-/- mice. PLoS One 2014;9:e99441.
48. Wenning C, Kloth C, Kuhlmann MT, et al. Serial F-18-FDG PET/CT distinguishes inflamed from stable plaque phenotypes in shear-stress induced murine atherosclerosis. Atherosclerosis 2014;234:276-82.
49. Rudd JH, Warburton EA, Fryer TD, et al. Imaging atherosclerotic plaque inflammation with [18F]-

fluorodeoxyglucose positron emission tomography. Circulation 2002;105:2708-11.
50. Masteling MG, Zeebregts CJ, Tio RA, et al. High-resolution imaging of human atherosclerotic carotid plaques with micro 18F-FDG PET scanning exploring plaque vulnerability. J Nucl Cardiol 2011;18:1066-75.
51. Menezes LJ, Kotze CW, Agu O, et al. Investigating vulnerable atheroma using combined (18)F-FDG PET/CT angiography of carotid plaque with immunohistochemical validation. J Nucl Med 2011;52:1698-703.
52. Hara M, Goodman PC, Leder RA. FDG-PET finding in early-phase Takayasu arteritis. J Comput Assist Tomogr 1999;23:16-8.
53. Blockmans D, Maes A, Stroobants S, et al. New arguments for a vasculitic nature of polymyalgia rheumatica using positron emission tomography. Rheumatology (Oxford) 1999;38:444-7.
54. Walter MA. [(18)F]fluorodeoxyglucose PET in large vessel vasculitis. Radiol Clin North Am 2007;45:735-44, viii.
55. Mochizuki Y, Fujii H, Yasuda S, et al. FDG accumulation in aortic walls. Clin Nucl Med 2001;26:68-9.
56. Yun M, Yeh D, Araujo LI, et al. F-18 FDG uptake in the large arteries: a new observation. Clin Nucl Med 2001;26:314-9.
57. Yun M, Jang S, Cucchiara A, et al. 18F FDG uptake in the large arteries: a correlation study with the atherogenic risk factors. Semin Nucl Med 2002;32:70-6.
58. Bucerius J, Duivenvoorden R, Mani V, et al. Prevalence and risk factors of carotid vessel wall inflammation in coronary artery disease patients: FDG-PET and CT imaging study. JACC Cardiovasc Imaging 2011;4:1195-205.
59. Paulmier B, Duet M, Khayat R, et al. Arterial wall uptake of fluorodeoxyglucose on PET imaging in stable cancer disease patients indicates higher risk for cardiovascular events. J Nucl Cardiol 2008;15:209-17.
60. Marnane M, Merwick A, Sheehan OC, et al. Carotid plaque inflammation on 18F-fluorodeoxyglucose positron emission tomography predicts early stroke recurrence. Ann Neurol 2012;71:709-18.
61. Kim HJ, Oh M, Moon DH, et al. Carotid inflammation on 18F-fluorodeoxyglucose positron emission tomography associates with recurrent ischemic lesions. J Neurol Sci 2014;347:242-5.
62. Moustafa RR, Izquierdo-Garcia D, Fryer TD, et al. Carotid plaque inflammation is associated with cerebral microembolism in patients with recent transient ischemic attack or stroke: a pilot study. Circ Cardiovasc Imaging 2010;3:536-41.
63. Müller HF, Viaccoz A, Fisch L, et al. 18FDG-PET-CT: an imaging biomarker of high-risk carotid plaques. Correlation to symptoms and microembolic signals. Stroke 2014;45:3561-6.
64. Rogers IS, Nasir K, Figueroa AL, et al. Feasibility of FDG imaging of the coronary arteries: comparison between acute coronary syndrome and stable angina. JACC Cardiovasc Imaging 2010;3:388-97.
65. Rudd JH, Myers KS, Bansilal S, et al. (18) Fluorodeoxyglucose positron emission tomography imaging of atherosclerotic plaque inflammation is highly reproducible: implications for atherosclerosis therapy trials. J Am Coll Cardiol 2007;50:892-6.
66. Worthley SG, Zhang ZY, Machac J, et al. In vivo non-invasive serial monitoring of FDG-PET progression and regression in a rabbit model of atherosclerosis. Int J Cardiovasc Imaging 2009;25:251-7.
67. Wu YW, Kao HL, Huang CL, et al. The effects of 3-month atorvastatin therapy on arterial inflammation, calcification, abdominal adipose tissue and circulating biomarkers. Eur J Nucl Med Mol Imaging 2012;39:399-407.
68. Tawakol A, Fayad ZA, Mogg R, et al. Intensification of statin therapy results in a rapid reduction in atherosclerotic inflammation: results of a multicenter fluorodeoxyglucose-positron emission tomography/computed tomography feasibility study. J Am Coll Cardiol 2013;62:909-17.
69. Fayad ZA, Mani V, Woodward M, et al. Safety and efficacy of dalcetrapib on atherosclerotic disease using novel non-invasive multimodality imaging (dal-PLAQUE): a randomised clinical trial. Lancet 2011;378:1547-59.
70. Nissen SE, Tardif JC, Nicholls SJ, et al. Effect of torcetrapib on the progression of coronary atherosclerosis. N Engl J Med 2007;356:1304-16.
71. Menezes LJ, Kayani I, Ben-Haim S, et al. What is the natural history of 18F-FDG uptake in arterial atheroma on PET/CT? Implications for imaging the vulnerable plaque. Atherosclerosis 2010;211:136-40.
72. Moses WW. Fundamental Limits of Spatial Resolution in PET. Nucl Instrum Methods Phys Res A 2011;648 Supplement 1:S236-S240.
73. Saha GB. Performance characteristics of PET scanners. Basics of PET imaging. New York: Springer Science. Available online: http://www.springer.com/cda/content/document/cda_downloaddocument/9781441908049-c3.pdf?SGWID=0-0-45-872146-p173949616
74. Demeure F, Hanin FX, Bol A, et al. A randomized trial on the optimization of 18F-FDG myocardial uptake suppression: implications for vulnerable coronary plaque

imaging. J Nucl Med 2014;55:1629-35.
75. Leide-Svegborn S. Radiation exposure of patients and personnel from a PET/CT procedure with 18F-FDG. Radiat Prot Dosimetry 2010;139:208-13.
76. Blau M, Nagler W, Bender MA. Fluorine-18: a new isotope for bone scanning. J Nucl Med 1962;3:332-4.
77. Blake GM, Park-Holohan SJ, Cook GJ, et al. Quantitative studies of bone with the use of 18F-fluoride and 99mTc-methylene diphosphonate. Semin Nucl Med 2001;31:28-49.
78. Eanes ED, Reddi AH. The effect of fluoride on bone mineral apatite. Metab Bone Dis Relat Res 1979;2:3-10.
79. Mick CG, James T, Hill JD, et al. Molecular imaging in oncology: (18)F-sodium fluoride PET imaging of osseous metastatic disease. AJR Am J Roentgenol 2014;203:263-71.
80. Piert M, Zittel TT, Becker GA, et al. Assessment of porcine bone metabolism by dynamic. J Nucl Med 2001;42:1091-100.
81. Rumberger JA, Simons DB, Fitzpatrick LA, et al. Coronary artery calcium area by electron-beam computed tomography and coronary atherosclerotic plaque area. A histopathologic correlative study. Circulation 1995;92:2157-62.
82. Demer LL, Tintut Y. Vascular calcification: pathobiology of a multifaceted disease. Circulation 2008;117:2938-48.
83. Wexler L, Brundage B, Crouse J, et al. Coronary artery calcification: pathophysiology, epidemiology, imaging methods, and clinical implications. A statement for health professionals from the American Heart Association. Writing Group. Circulation 1996;94:1175-92.
84. New SE, Aikawa E. Molecular imaging insights into early inflammatory stages of arterial and aortic valve calcification. Circ Res 2011;108:1381-91.
85. Aikawa E, Nahrendorf M, Figueiredo JL, et al. Osteogenesis associates with inflammation in early-stage atherosclerosis evaluated by molecular imaging in vivo. Circulation 2007;116:2841-50.
86. Nadra I, Mason JC, Philippidis P, et al. Proinflammatory activation of macrophages by basic calcium phosphate crystals via protein kinase C and MAP kinase pathways: a vicious cycle of inflammation and arterial calcification? Circ Res 2005;96:1248-56.
87. Derlin T, Richter U, Bannas P, et al. Feasibility of 18F-sodium fluoride PET/CT for imaging of atherosclerotic plaque. J Nucl Med 2010;51:862-5.
88. Derlin T, Wisotzki C, Richter U, et al. In vivo imaging of mineral deposition in carotid plaque using 18F-sodium fluoride PET/CT: correlation with atherogenic risk factors. J Nucl Med 2011;52:362-8.
89. Derlin T, Tóth Z, Papp L, et al. Correlation of inflammation assessed by 18F-FDG PET, active mineral deposition assessed by 18F-fluoride PET, and vascular calcification in atherosclerotic plaque: a dual-tracer PET/CT study. J Nucl Med 2011;52:1020-7.
90. Li Y, Berenji GR, Shaba WF, et al. Association of vascular fluoride uptake with vascular calcification and coronary artery disease. Nucl Med Commun 2012;33:14-20.
91. Beheshti M, Saboury B, Mehta NN, et al. Detection and global quantification of cardiovascular molecular calcification by fluoro18-fluoride positron emission tomography/computed tomography--a novel concept. Hell J Nucl Med 2011;14:114-20.
92. Dweck MR, Chow MW, Joshi NV, et al. Coronary arterial 18F-sodium fluoride uptake: a novel marker of plaque biology. J Am Coll Cardiol 2012;59:1539-48.
93. Kurata S, Tateishi U, Shizukuishi K, et al. Assessment of atherosclerosis in oncologic patients using ^{18}F-fluoride PET/CT. Ann Nucl Med 2013;27:481-6.
94. Janssen T, Bannas P, Herrmann J, et al. Association of linear ^{18}F-sodium fluoride accumulation in femoral arteries as a measure of diffuse calcification with cardiovascular risk factors: a PET/CT study. J Nucl Cardiol 2013;20:569-77.
95. Blomberg BA, Thomassen A, Takx RA, et al. Delayed sodium 18F-fluoride PET/CT imaging does not improve quantification of vascular calcification metabolism: results from the CAMONA study. J Nucl Cardiol 2014 ;21:293-304.
96. Joshi NV, Vesey AT, Williams MC, et al. 18F-fluoride positron emission tomography for identification of ruptured and high-risk coronary atherosclerotic plaques: a prospective clinical trial. Lancet 2014;383:705-13.
97. Morbelli S, Fiz F, Piccardo A, et al. Divergent determinants of 18F-NaF uptake and visible calcium deposition in large arteries: relationship with Framingham risk score. Int J Cardiovasc Imaging 2014;30:439-47.
98. Fiz F, Morbelli S, Piccardo A, et al. 18F-NaF Uptake by Atherosclerotic Plaque on PET/CT Imaging: Inverse Correlation Between Calcification Density and Mineral Metabolic Activity. J Nucl Med 2015;56:1019-23.
99. Dweck MR, Jenkins WS, Vesey AT, et al. 18F-sodium fluoride uptake is a marker of active calcification and disease progression in patients with aortic stenosis. Circ Cardiovasc Imaging 2014;7:371-8.
100. García-García HM, Mintz GS, Lerman A, et al. Tissue characterisation using intravascular radiofrequency data

analysis: recommendations for acquisition, analysis, interpretation and reporting. EuroIntervention 2009;5:177-89.
101. Ehara S, Kobayashi Y, Yoshiyama M, et al. Coronary artery calcification revisited. J Atheroscler Thromb 2006;13:31-7.
102. Irkle A, Vesey AT, Lewis DY, et al. Identifying active vascular microcalcification by (18)F-sodium fluoride positron emission tomography. Nat Commun 2015;6:7495.
103. Mauriello A, Servadei F, Zoccai GB, et al. Coronary calcification identifies the vulnerable patient rather than the vulnerable Plaque. Atherosclerosis 2013;229:124-9.
104. Puri R, Nicholls SJ, Shao M, et al. Impact of statins on serial coronary calcification during atheroma progression and regression. J Am Coll Cardiol 2015;65:1273-82.
105. Shaw LJ, Narula J, Chandrashekhar Y. The never-ending story on coronary calcium: is it predictive, punitive, or protective? J Am Coll Cardiol 2015;65:1283-5.
106. Hutcheson JD, Maldonado N, Aikawa E. Small entities with large impact: microcalcifications and atherosclerotic plaque vulnerability. Curr Opin Lipidol 2014;25:327-32.

Cite this article as: Scherer DJ, Psaltis PJ. Future imaging of atherosclerosis: molecular imaging of coronary atherosclerosis with 18F positron emission tomography. Cardiovasc Diagn Ther 2016;6(4):354-367. doi: 10.21037/cdt.2015.12.02

